Technical Paper
Int'l J. of Aeronautical & Space Sci. 13(2), 221–228 (2012)
DOI:10.5139/IJASS.2012.13.2.221

IJASS
International Journal of Aeronautical and Space Sciences

Feasibility Study to Actively Compensate Deformations of Composite Structure in a Space Environment

Ciro Farinelli*
Department of aerospace engineering, Politecnico di Milano, Italy

Hong-Il Kim**
Department of aerospace engineering, KAIST, South Korea

Jae-Hung Han***
Department of aerospace engineering, KAIST, South Korea

Abstract

An active compensation method for the deformation of composite structures using additional controllable metal parts is proposed, and its feasibility is experimentally investigated in a simulated space environment. Composite specimens are tested in a vacuum chamber, which is able to maintain pressure on the order of 10-3 torr and interior temperature in the range of ±30 ˚C. The displacement-measuring interferometer system, which consists of a heterodyne HeNe laser and an interferometer, is used to measure the displacement of the whole structure. Meanwhile, the strain of the composite part and temperature of both parts are measured by fiber Bragg grating sensors and thermistors, respectively. The displacement of the composite structure is maintained within a tolerance of ±1 μm by controlling the elongation of the metal part, which is bonded to the end of the composite part. Also, the possibility of fiber Bragg grating sensors as control input sensors is successfully demonstrated using a proper corrective factor based on the specimen temperature gradient data.

Key words: composite structure, dimensional stability, coefficient of thermal expansion (CTE), fiber Bragg grating (FBG) sensors, displacement measuring interferometer (DMI), space environment.

1. Introduction

In the past years, the dimensional stability problem has been one of the big issues for optomechanical space structures. Thanks to various innovations in materials and precise analysis and control, the limits of the structure's stability have gradually increased [1].

High-dimensional-stability devices show significant performance degradation due to misalignment phenomena. In optical devices or high-accuracy measurement systems, the relative position and alignment between two optical components like mirrors and sensors should be maintained. There are three representative types of misalignment between two optical components: 1) the *tilt* when the relative orientation is different, 2) the *decenter* when the axis of one of the components presents an offset from those of the other elements, and 3) the *despace* when the distance between the two components changes. It is crucial to reduce these effects by a determined tolerance [2]. The most substantial destabilizing factors in the space optical devices are vibrations, ambient

* Graduate student, E-mail : ciro.farinelli@mail.polimi.it
** Researcher, Ph. D.
*** Professor, Corresponding author
E-mail : jaehunghan@kaist.ac.kr

Received: June 6, 2012 Accepted: June 29, 2012

http://ijass.org pISSN: 2093-274x eISSN: 2093-2480

microgravity, ionizing radiation of the Earth's natural radiation, and variations in temperature [3].

In this study, the effects of temperature variation on dimensional changes are considered, and an active compensation method for the deformation of composite structures using an additional controllable metal part is proposed. The feasibility of the method is experimentally investigated in a simulated space environment.

1.1 State of art

Hull [4] utilized semi-active focus and thermal compensation of a centrally obscured reflective telescope using a system of heating tapes and thermal sensors on a telescope. The principle is to maintain the temperature of the system within a range where the dimensional stability is defined. Piezoelectric (PZT) actuators were also used to compensate for composite beam deformations [5], and the range of displacement control was on the order of 1 mm. Dano and Julliere [6] used a Macro-Fiber Composite (MFC) actuator to compensate the thermal distortion in composite structures made of four layers: one layer made by PZT fibers and epoxy, one layer by epoxy, one layer by copper electrodes and epoxy and one layer by Kapton. In the study by Savitskii [7], material with a negative coefficient of thermal expansion (CTE) was associated to material with positive CTE in order to passively compensate the deformations caused by the temperature. Unfortunately, this solution is only valid only within a relative small temperature range because the CTE is not constant at different temperatures. Cordero *et al*. [8] focused on characterizing dimensionally ultra-stable materials. The instrument used for this purpose is a high-precision dilatometer. Its accuracy is at best ±0.1 × 10-6 ℃$^{-1}$ for data obtained over 100 ℃. They used Peltier elements to change the temperature of the system and reached a dimensional stability tolerance of ±1 nm. Giesen and Folgering [9] developed optical delay lines and combined piezo effects with structures of different CTE materials. Moreover their paper described principles to minimize thermal disturbance of optical performance.

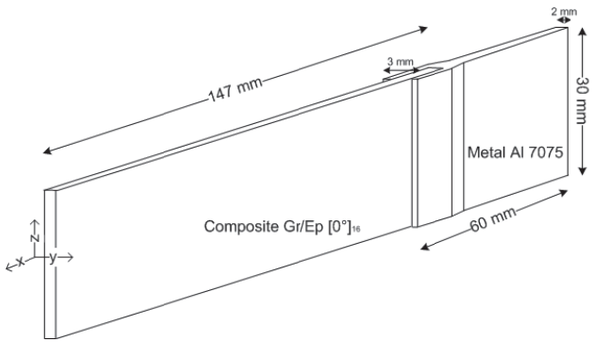

Fig. 1. Concept and dimensions of the specimen. The metal and the composite part were bonded by double lap layer bonding method, using Epoxy glue. X is the longitudinal axis.

1.2 Proposed solution

Though there have been various ideas proposed for precise dimensional controls, a space-realizable sensor system needs to be implemented. The proposed solution provides a dimensionally stable structure system that actively compensates for dimensional changes in a space environment. The system consists of a composite part, a metal part, FBG sensors, and a heater. When the dimensions of the composite are changed by temperature variation, FBG sensors define deformation of the whole system by the punctual strain. Then the heater provides thermal expansion of the metal part, which compensates for deformation of the composite. A displacement-measuring interferometer (DMI)

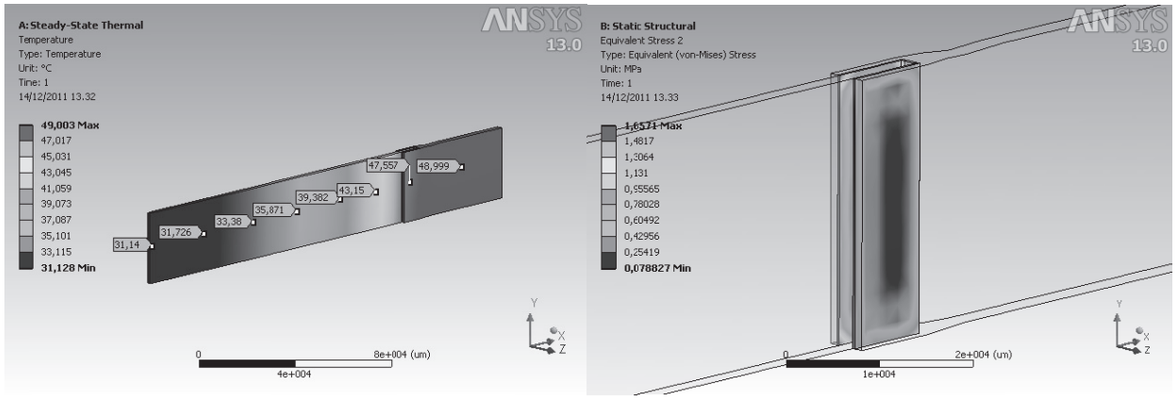

Fig. 2. Finite element model. Temperature of the whole system (left), detail of Von Mises stress of the epoxy glue in the double lap bonding method configuration (right).

DOI:10.5139/IJASS.2012.13.2.221

system that can measure the entire displacement of the specimen is used to validate the feasibility of the proposed solution.

2. Experimental

2.1 Description of the specimen

The specimen dimensions and the allowable tolerance in displacements were chosen by referring to the references concerning real space structures and space telescopes [7, 10, 11]. The dimensional stability tolerance was chosen to be ±3 μm for an ambient temperature variation of ±8℃. Note that the balance between the controllable thermal deformation and the mechanical stiffness and strength should also be considered.

Fig. 1 shows the dimensions and the shape of the whole specimen chosen in this study, respecting constraints of the vacuum chamber used in this study. Concerning the shape, it was decided to design an oblong specimen to focus the behaviour along one axis, and to facilitate the installation of the specimen on the support of the vacuum chamber. The z-direction (gravity direction) dimension was imposed on 30 mm to have enough stiffness along this direction to avoid eventual deformations caused by the gravity field.

The composite part used in this study was $[0^\circ]_{16}$ Gr/Ep, unidirectional along the longitudinal axis, along which its CTE was -0.81×10^{-6} K^{-1}. Al 7075 was employed as the metal part, and its CTE value was 23.6×10^{-6} K^{-1}. CTE values defined in (1) were measured following the method of Kim *et al.* [12].

$$CTE = \frac{1}{L_0}\frac{\Delta L}{\Delta T} = \frac{\left(\frac{\Delta L}{L_0}\right)}{\Delta T} = \frac{\varepsilon}{\Delta T} \tag{1}$$

where $\Delta L = L_1 - L_2$ and $\Delta T = T_1 - T_2$.

The metal part and the composite part were bonded together by the double lap layer bonding method, using epoxy glue. This choice was made to enable enough stiffness to bear stress due to the difference of temperature and CTEs of metal and composite parts, and to thermally isolate the materials as much as possible. The thickness of both layers of epoxy glue was 0.5 mm. This was chosen after a finite element analysis on the specimen.

A series of finite element analyses were conducted to predict the temperature distributions, the degree of dimensional controllability, and to verify the structural integrity. In the FE analyses, the end of the metal part was fixed. Fig. 2 shows the steady-state temperature distribution and the corresponding stress distribution for a 50 ℃ temperature on the heater surface of the metal part was imposed, with an environmental temperature of 21 ℃. Within 1 hour, the composite part reached the temperature of 31 ℃. The results of the FE analysis in Fig. 2 also show that the maximum Von Mises stress of the epoxy glue is 1.9 MPa, far below the yield compressive strength of 36 MPa.

2.2 DMI system

Interferometers are able to measure displacements without contacting the specimens controlling the environmental and geometrical error sources [13]. The DMI system is composed of a dual-mode laser head that generates HeNe laser light at a 633 nm wavelength at 3.4 and 4.0 MHz, with highly stable interferometers, reflectors, fiber optic pickups and supporting electronics. The laser consists of two beams orthogonally polarized. Two beams travel along the reference path within the interferometer and the measurement path. The length difference between the two paths induces the phase difference $\Delta\varphi$ as shown in the following:

$$\Delta\varphi \simeq 2\pi M(d_A - d_B)/\lambda_A \tag{2}$$

where M is the number of passes the laser makes through the interferometer (M=2), λ_A is the wavelength of the laser A, and d_A and d_B are the lengths of the reference path and measurement path, respectively.

The displacement of the target (x=d_A–d_B) is obtained by measuring the phase difference $\Delta\varphi$. The relation that correlates the phase difference $\Delta\varphi$ to the frequency shift f (Doppler frequency shift) measured by the DMI system is expressed as follows, by the time differentiation of $\Delta\varphi$:

$$\Delta f = M\, df = \frac{M}{2\pi}\frac{d\varphi}{dt} = \frac{Mv}{\lambda} \tag{3}$$

where v is the target velocity. In order to calculate the frequency shift f, the initial frequencies from the laser head and the changed frequencies from the interferometer are collected in the receiving electronics consisting of a phase meter, an integrator and so on. The target velocity v is calculated using the frequency shift data f from the phase meter. Then, the displacement is obtained by summing v.

2.3 FBG

The FBG sensor is a type of fiber optic sensor, its use in space structures is being actively studied. The working principle of the FBG is based on a periodic change of the refractive index in the optical fiber. Each FBG reflects a specific wavelength (Bragg wavelength λ_B). The optical fiber

used for the FBG sensor has its own CTE α_f and thermo-optic coefficient ξ_f so that the temperature effects should be compensated to measure the pure specimen strain, as in the following description based on the work of Lo and Chuang [14]. When the FBG sensor is attached to the specimen with a temperature change ΔT, the Bragg wavelength's shift of the attached FBG sensor can be expressed as the sum of the mechanical strain resulting from specimen strain ε_s, and the temperature variation ΔT in the FBG sensor, as it is expressed as follows:

$$\left(\frac{\Delta\lambda_B}{\lambda_B}\right)_G = (1-p_e)\cdot\varepsilon_s + \\ +\left[\xi_f + n_e^2(2p_{12}+p_{11})\alpha_f\right]\cdot\Delta T \tag{4}$$

where the term pe is the photo-elastic constant of the optical fiber. p11 and p12 are the components of the strain-optic tensor, and ne is the effective refractive index of the Bragg grating.

The specimen strain ε_s consists of a mechanical strain ε_m and a thermal strain expressed as follows:

$$\varepsilon_s = \varepsilon_m + \alpha_s\,\Delta T \tag{5}$$

where α_s is the coefficient of thermal expansion of the specimen. Substituting the value of ε_s in (4), we obtain:

$$\left(\frac{\Delta\lambda_B}{\lambda_B}\right)_G = (1-p_e)\cdot(\varepsilon_m + \alpha_s\,\Delta T) + \\ +\left[\xi_f + n_e^2(2p_{12}+p_{11})\alpha_f\right]\cdot\Delta T \tag{6}$$

For the free FBG sensor (floating on the specimen), no specimen strain ε_s is transmitted to the FBG sensor. Therefore, the Bragg wavelength's shift in the free FBG sensor can be expressed erasing the first terms:

$$\left(\frac{\Delta\lambda_B}{\lambda_B}\right)_F = \left[\xi_f + n_e^2(2p_{12}+p_{11})\alpha_f\right]\cdot\Delta T \tag{7}$$

The compensation for the temperature effect on the FBG sensor is achieved by subtracting the two relations above:

$$\left(\frac{\Delta\lambda_B}{\lambda_B}\right)_G - \left(\frac{\Delta\lambda_B}{\lambda_B}\right)_F = (1-p_e)\cdot(\varepsilon_m + \alpha_s\,\Delta T) \tag{8}$$

If there are no external loads, the mechanical strain ε_m becomes zero. To obtain the value of the strain from the differentiation of the wavelength of the FBG sensors, it is mandatory to define the constant p_e. The relation to have this constant is as expressed follows:

$$p_e = 1 - \frac{\left(\frac{\Delta\lambda_B}{\lambda_B}\right)_G - \left(\frac{\Delta\lambda_B}{\lambda_B}\right)_F}{\varepsilon_T} \tag{9}$$

where

$$\varepsilon_T = \alpha_s\,\Delta T = \frac{\Delta L}{L_0} \tag{10}$$

This depends exclusively on the temperature behaviour of the specimen because no mechanical stress is imposed. The value of ΔL is defined by the DMI system, and L_0 is the initial length of the system. The reference frequencies of wavelengths come from the average of values obtained for 20 minutes at the sample frequency of 0.1 Hz in the thermal and pressure static conditions inside of the vacuum chamber. In this research, pe is 0.305, and the reference frequencies of the attached FBG ($\lambda_{ref}G$) and floating FBG ($\lambda_{ref}F$) are 1553.2080 Hz and 1547.1556 Hz, respectively.

2.4 Specimen setup

Concerning the heating tape, the resistance per length is 28 Ω/ft, and the maximum allowable power per length is 70 W/ft. It was attached on the metal part surface in one row, on both faces. The heating tape contained 4 resistive wires, embedded in 11-mm-width tape, heating the surface quasi-isotropically. Fig. 3 explains the connection configuration of the heating tape. The parts, where the tape deflects from up to down, were covered with isolating tape. The little square in the centre was cut out in order to facilitate attaching the thermistor.

FBG sensor arrays can be easily prepared by connecting several Bragg gratings written at different wavelengths in a line along the length of a single fiber and addressing each sensor individually using wavelength division multiplexing (WDM) technology. In this case, an array of two Bragg gratings was created. As Fig. 4 shows, the first Bragg grating (*FBG_glued*) was completely glued at the surface of the composite. The second Bragg grating (*FBG_floating*) was attached just in one point in order to be affected just by temperature variations. Then, the fibers were covered by a

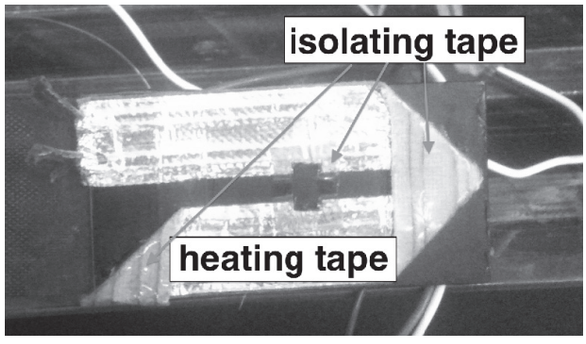

Fig. 3. Heating tape configuration on metal part.

DOI:10.5139/IJASS.2012.13.2.221

Multi-Layer Isolator (MLI). The orientation of the attached FBG should be along the longitudinal axis of the composite material.

The thermistors are TO-92 Plastic Package from the LM35 series by the National Semiconductor. It does not require any external calibration or trimming to provide typical accuracies of ±0.25 ℃ at room temperature and ±0.75 ℃ over a full -55 ~ 150 ℃ temperature range. They were attached on specified points: the first one at 20 mm from the end of the composite part, the second one at 30 mm from the metal part and the third one in the center of the metal part, as depicted in Fig. 5. These thermistors are called T1, T2 and T3, respectively. T3 was isolated from the heating tape with a layer of isolating tape. Between the thermistors and the surface of the specimen, a layer of thermal conductive foam was used.

2.5 Experiment setup

The DMI system consists of a laser head (Agilent 5517D), two plane mirror interferometers (Agilent 10706B high-stability plane mirror interferometer), a specimen base with a reference mirror, a receiver (Agilent E1708A remote dynamic receiver) and a PCI laser board (Agilent N1231B). The entire experimental setup was maintained inside of a vacuum chamber simulating the space environment in terms of pressure (on the order of 10-3 torr) and variations of temperature (±10 ℃ in about 2 hours). Since the specimen was laid on the specimen base, the base was supported by a roller to let the specimen float with minimal friction.

Fused silica was selected as the material for the specimen base, specimen roller and reference mirror because of its very small CTE (on the order of 10–7 $℃^{-1}$). One end of the specimen was attached to the reference mirror to compensate for the specimen base's expansion. The heating tape was connected through the optical feed-through to the power supply regulator.

The temperature of the metal part was detected with thermistor T3, and the temperature of the composite part was detected by an average of T1 and T2. All data from the DMI system, FBG sensors and thermistors were collected using a LabVIEW computer (NI PXI 8186). Fig. 6 shows the overall experimental setup scheme. The interferometers and the specimen base were placed inside the vacuum chamber. The laser head and receiver were located outside the chamber. The quartz window was installed on the vacuum chamber

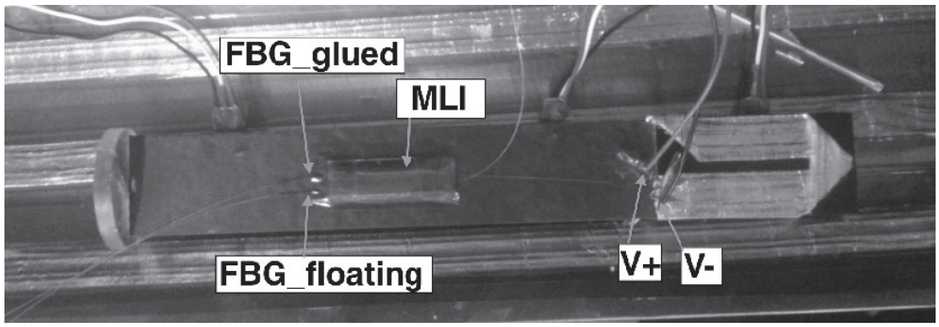

Fig. 4. Front side of the specimen. FBG attachment configuration. The FBG_floating is attached to the composite part just in one point, the FBG_ glued is completely glued to surface. Positive and negative connections of heating tape.

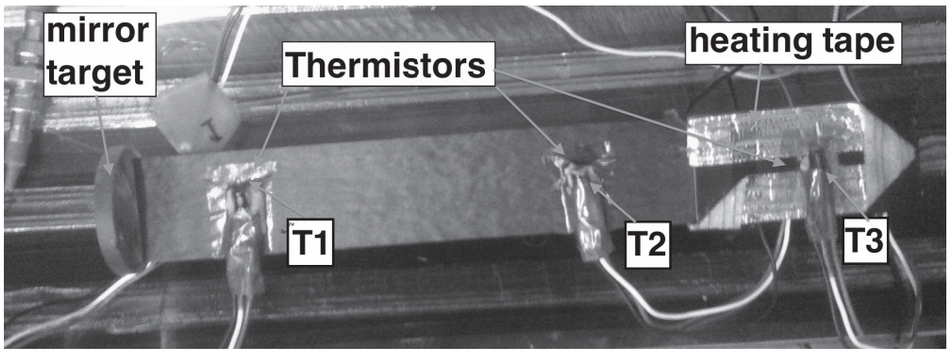

Fig. 5. Opposite side of the specimen. Thermistor attachment configuration. A layer of thermo-conductive foam was created between the sensors and the specimen. The thermistors attachment points are: T1 at 20 mm from the left side, T2 at 30 mm from the metal part, T3 at 25 mm from the right side.

to let the laser light pass through. A heat tunnel, which surrounded the specimen and specimen base, was coated in black to easily transfer heat through radiation.

3. Results

In order to facilitate the lab-scale dimensional controls, the experiment was performed in always-positive heat power delivery mode. The metal part was heated by the heating tape; and the cooling control of both parts was performed by radiation. Therefore, the temperature of the metal part was set to be higher than the ambient temperatures. The gap shall be enough to keep the temperature of the metal part higher than the composite temperature during the entire experiment, allowing the heat power of the system transferring outward by radiation during the cooling phase. Fig. 7 shows the typical temperature time course of the specimen. The vacuum chamber temperature range was set to 30~46 ℃. The initial temperature of the vacuum chamber and composite part was set at 38 ℃, and the initial temperature of the metal part was set at 47 ℃. As shown in Fig. 7, the temperature of the metal part was set to 9 ℃ higher than ambient temperature to increase the controllability of the displacement by adjusting the voltage of the heaters during the control. The voltage range used to control the displacement of the metal part was 0~6 V. The temperature of the composite part was the control input of the heating system. The control input was the displacement measured by the DMI system shown in Fig. 6, defined as the variation of the initial elongation of the whole specimen and the elongation during the experiment. The control output was the voltage, manipulated by the power supply in steps of 0.05 V. Control time sampling was at 1 sample per 1 minute. The minimum variation of voltage between two subsequent values was 0.1 V.

Fig. 8 clearly shows that the deformation measured by the DMI system was maintained within the tolerance of ±1 μm, which satisfies the goal of dimensional stability tolerance of ±3 μm.

Because the bonding was not thermally isolated between both parts, a temperature gradient existed along the longitudinal direction of the specimen as shown on the left side of Fig. 2. Thus, the direct integration of strain measured by FBG was not the whole displacement of the specimen which could be measured by the DMI system. Therefore, a corrective factor with respect to the temperature difference between the composite part T_{comp} and the initial temperature T_{ref} was introduced to calibrate the specimen displacement with the strains by FBG sensors. The corrective factor is approximated as in (11).

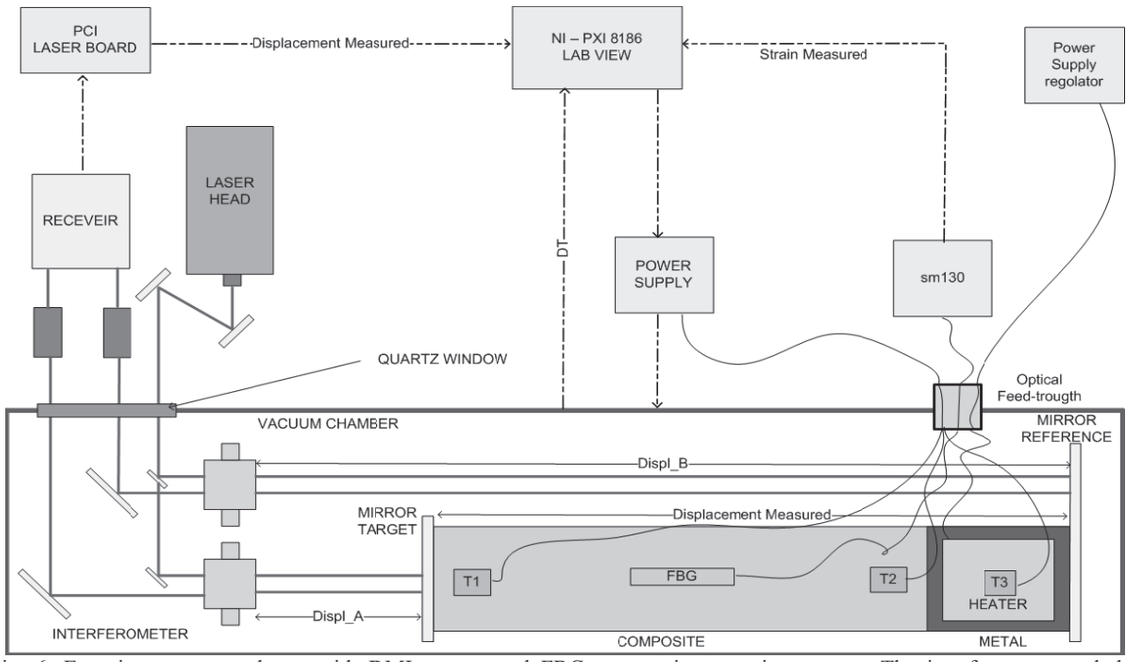

Fig. 6. Experiment setup scheme with DMI system and FBG sensors interrogation system. The interferometer and the specimen were located in the vacuum chamber while the laser heat and electronics for the DMI and FBG sensors and power deliver for heating tape were outside. Laser light passed through the quartz windows and the FBG sensors and heating tape were connected using a feed-through.

DOI:10.5139/IJASS.2012.13.2.221

$$C_f = A \cdot \left(T_{comp} - T_{ref}\right) + B \tag{11}$$

where A=-1.3×10^{-5} K^{-1} and B=-2.5×10^{-6} are the constants of the approximating function.

This function shall be applied to the strains by the FBG sensor. Fig. 9 shows the behaviour of the corrective factor. Fig. 10 shows that the controlled displacement based on the FBG sensors with the corrective factor remained within the tolerance of ±1 μm. Without corrective factor, the small displacement was hardly measured by using only FBG sensors. Thus, the proper corrective factor should be applied to the FBG sensors in order to use the strain data from FBG sensors as the control input.

4. Conclusions

An active dimension compensation concept for a composite structure using an additional controllable metal part was demonstrated.

From the FEM analysis, proper specimen configuration was designed. The dimensional changes of the specimen were engaged in a vacuum chamber in order to simulate space conditions, and these dimensional changes were compensated by proper control of the temperature of the metal part. From the test, it has been shown that dimensional stability of ±1 μm was successfully achieved. In addition, the corrective factor calculated from the temperature data showed the possibility of using the FBGs as a monitoring sensor for dimensional stability.

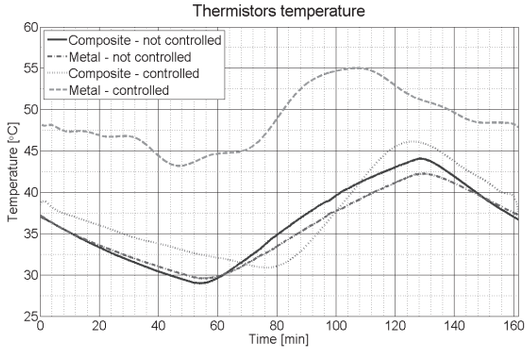

Fig. 7. Specimen temperature

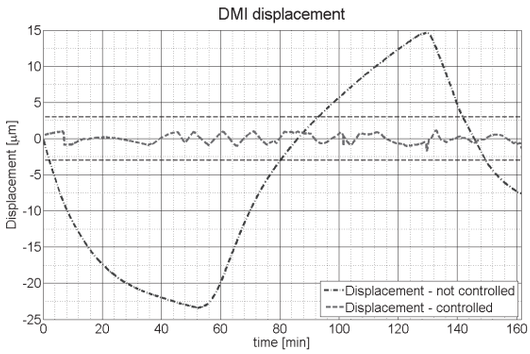

Fig. 8. Controlled displacement based on the DMI data.

References

[1] Wolff E. G., *Introduction to dimensional stability of composite materials*, Destech Publications, Lancaster, PA, 2004.

[2] URL: http://www.telescope-optics.net [cited 17 October 2011]

[3] Danilov V. A., Lysenko A. I., Malamed E. R. and Sokol'skii M. N., "Service systems of space telescopes", *Opticheskii Zhurnal*, Vol. 69, 2002, pp. 36-44.

[4] David A. H., "Semi-active focus and thermal compensation of centrally obscured reflective telescope", *United States Patent*, US 6404547, 2002.

[5] Song G., Zhou X. and Binienda W., "Thermal deformation compensation of a composite beam using

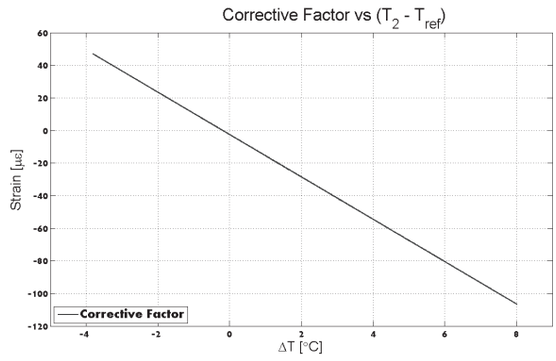

Fig. 9. Corrective factor

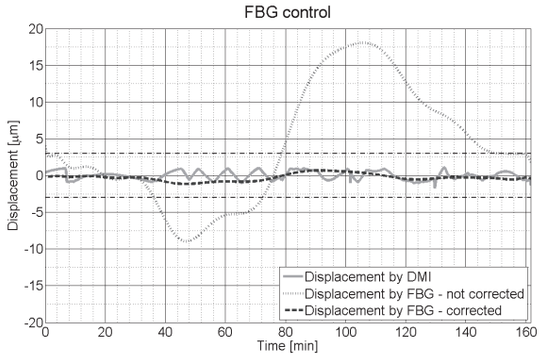

Fig. 10. Controlled displacement based on the FBG data with corrective factor.

piezoelectric actuators", *Smart materials and structures*, Vol. 13, No. 1, 2004, pp. 30-37.
doi:10.1088/0964-1726/13/1/004

[6] Dano M. L. and Julliere B., "Active control of thermally induced distortion in composite structures using Macro fiber composite actuators", *Smart materials and structures*, Vol. 16, No. 6, 2007, pp. 2315-2322.
doi:10.1088/0964-1726/16/6/035

[7] Savitskii A. M., "How the thermal regime affects the structural characteristics of a space telescope", *Journal of Optical Technology*, Vol. 76, No. 10, 2009, pp. 662-665.
http://dx.doi.org/10.1364/JOT.76.000662

[8] Cordero J., Heinrich T., Shuldt T., Gohlke, M, Lucarelli S., Weise D., Johann U. and Braxmaier C., "Interferometry based high-precision dilatometry for dimensional characterization of high stable materials", *Measurement Science and Technology*, Vol. 20, No. 9, 2009, pp. 1-10.
doi:10.1088/0957-0233/20/9/095301

[9] Giesen, P. and Folgering, E., "Design guidelines for thermal stability in optomechanical instruments", *Proceedings of SPIE Optomechanics*, Vol. 5176, 2003, pp. 126-134.

[10] Yoshinori S., Kiyoshi I., Yukio K., Saku T., and Toshifumi S., "Instrument design and on-orbit performance of the solar optical telescope aboard hinode (Solar-B)", *Bulletin of the American Astronomical Society*, Vol. 39, 2008, pp. 197-220.

[11] Krim M. H., "Design of highly stable optical support structure", *Optical engineering*, Vol. 14, No. 6, 1975, pp. 552-558.

[12] Kim H.-I., Yoon J.-S., Kim H.-B. and Han J.-H., "Measurement of the thermal expansion of space structure using fiber Bragg grating sensors and displacement measuring interferometers", *Smart materials and structures*, Vol. 21, No. 8, 2010, pp. 1-8.
doi:10.1088/0957-0233/21/8/085704

[13] *Laser and Optics User's Manual: Standard Optics and Assemblies*, Agilent Technology, Santa Clara, CA, 2002

[14] Lo Y.-L. and Chuang H. S., "Measurement of thermal expansion coefficients using an in-fibre Bragg-grating sensor", *Measurement Science and technology*, Vol. 9, No. 9, 1998, pp. 1543-1547.
doi:10.1088/0957-0233/9/9/025